

Electronic Supplementary Information

Selective fluorescent probe for Tl³⁺ ions through metal-induced hydrolysis and its application for direct assay of artificial urine

Myung Gil Choi, Yerin Jang, Mi Gang Kim, Sangdoo Ahn* and Suk-Kyu Chang*

Department of Chemistry, Chung-Ang University, Seoul 06974, Republic of Korea

Contents

Experimental details

Table S1. Representative Tl³⁺ signaling sensors and reaction-based probes reported previously

Table S2. Photophysical properties of **TP-1** and **TP-2** in the presence and absence of Tl³⁺ ions

Fig. S1. UV-vis spectra of (a) **TP-1** and (b) **TP-2** in the presence and absence of Tl³⁺.

Fig. S2. Time-dependent fluorescence emission of **TP-1** at 443 nm in response to Tl³⁺.

Fig. S3. Time-dependent fluorescence emission of **TP-2** at 455 nm in response to Tl³⁺.

Fig. S4. Changes in fluorescence intensity enhancement (I/I_0) at 443 nm of **TP-1** in the presence of common anions. Inset: fluorescence spectra of **TP-1**.

Fig. S5. Changes in fluorescence intensity ratio ($I_{\text{anion+Tl(III)}}/I_{\text{Tl(III)}}$) of **TP-1** at 443 nm in the presence of coexisting anions.

Fig. S6. Changes in fluorescence intensity enhancement (I/I_0) of **TP-1** at 443 nm in the presence of urine components.

Fig. S7. Partial ¹H NMR spectra of (a) **TP-1**, (b) **TP-1** + Tl³⁺, and (c) 2-acetyl-6-methoxynaphthalene in DMSO-*d*₆.

Fig. S8. Mass spectrum of the Tl³⁺ signaling product of **TP-1**.

- Fig. S9.** TLC profile of **TP-1** (spot A), **TP-1** with Tl³⁺ (2.0 eq.) (spot B), and 2-acetyl-6-methoxynaphthalene (spot C).
- Fig. S10.** Effect of pH on the Tl³⁺ signaling of **TP-1** expressed by changes in fluorescence intensity at 443 nm.
- Fig. S11.** Stability of **TP-1** stock solution over different storage durations.
- Fig. S12.** ¹H NMR spectrum of **TP-1** in DMSO-*d*₆ (600 MHz).
- Fig. S13.** ¹³C NMR spectrum of **TP-1** in DMSO-*d*₆ (150 MHz).
- Fig. S14.** HSQC NMR spectrum of **TP-1** in DMSO-*d*₆.
- Fig. S15.** HMBC NMR spectrum of **TP-1** in DMSO-*d*₆.
- Fig. S16.** High-resolution mass spectrum of **TP-1**.
- Fig. S17.** HPLC chromatogram of **TP-1**.
- Fig. S18.** ¹H NMR spectrum of **TP-2** in DMSO-*d*₆ (600 MHz).
- Fig. S19.** ¹³C NMR spectrum of **TP-2** in DMSO-*d*₆ (150 MHz).
- Fig. S20.** High-resolution mass spectrum of **TP-2**.
- Fig. S21.** HPLC chromatogram of **TP-2**.

Experimental details

1. General

Fluorophores 2-acetyl-6-methoxynaphthalene and 6-methoxy-2-naphthaldehyde were purchased from Tokyo Chemical Industry Co. (TCI). Hydrazine monohydrate was obtained from Yakuri Pure Chemicals Co. NMR (^1H and ^{13}C) spectra were measured using a Varian VNS NMR spectrometer. High-resolution mass spectrometry (HRMS) was conducted using a JEOL JMS-700 mass spectrometer with electron ionization (EI). UV-vis and fluorescence spectra were measured using Scinco S-3100 and FS-2 spectrophotometers, respectively.

Table S1. Representative Tl^{3+} signaling sensors and reaction-based probes reported previously

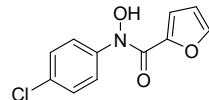
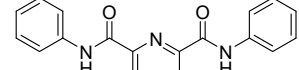
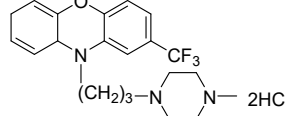
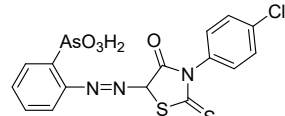
Structure	Signal	Conditions	Mechanism	LOD	Application	Merit	Ref.
	Colorimetry	pH 7.0 aqueous solution with 0.1% acetonitrile	Tl^{3+} -hydroxamic acid complex formation	-	Tl^{3+} assay in standard samples	• Naked eye detection	S1
	Colorimetry	Glycine-HCl buffer (pH 1.0)	Tl^{3+} -2,6-bis(<i>N</i> -phenyl carbamoyl)pyridine complex formation	1.2 nM (pre-concentration)	Tl^{3+} assay in environmental and biological samples	• Naked eye detection • High sensitivity	S2
	Colorimetry	H_2PO_4 solution	Oxidation of trifluoperazine	26,000 nM	Tl^{3+} assay in environmental and biological samples	• Naked eye detection • Biological application	S3
	Fluorescence	Acetone containing 10% HCl	Oxidation of arsenoxylphenylazo rhodanine	0.0013 nM (pre-concentration)	Tl^{3+} assay in environmental samples	• High sensitivity	S4

Table S1. Representative Tl^{3+} signaling sensors and reaction-based probes reported previously (*continued*)

Structure	Signal	Conditions	Mechanism	LOD	Application	Merit	Ref.
	Colorimetry	H_2PO_4 solution	Oxidative coupling of MBTH and IDH	72,000 nM	Tl^{3+} assay in environmental and biological samples	• Naked eye detection • Biological application	S5
	Colorimetry, Fluorescence	pH 4.76 acetate buffer with 20% (v/v) DMSO	Hydrolysis of sulfonhydrazide	190 nM	Tl^{3+} assay in commercial reagent using office scanner	• Naked eye detection • IT-device-based technique	S6
	Colorimetry, Fluorescence	pH 4.2 acetate buffer with 30% (v/v) DMSO	Hydrolysis of hydroxamate	290 nM	Tl^{3+} assay in biological samples using smartphone	• Naked eye detection • Biological application • IT-device-based technique	S7
	Fluorescence	pH 4.8 acetate buffer with 1% (v/v) DMF	Hydrolysis of hydrazone	19 nM	Tl^{3+} assay in biological samples using smartphone	• High sensitivity • Biological application • IT-device-based technique	This work

Table S2. Photophysical properties of **TP-1** and **TP-2** in the presence and absence of Ti^{3+} ions

	Maximum λ_{abs} (nm)	Molar extinction coefficient (ϵ) ($\text{cm}^{-1}\text{M}^{-1}$)	Maximum λ_{em} (nm)	Quantum yield (Φ)^[a]
TP-1 only	292	14,704	435	0.011
TP-1 + Ti³⁺	310	11,256	443	0.33
TP-2 only	306	19,682	436	0.015
TP-2 + Ti³⁺	315	10,974	455	0.20

[a] Fluorescence quantum yields were measured by comparing with anthracene as a reference ($\Phi_{\text{anthracene}} = 0.27$, ethanol).⁸⁸

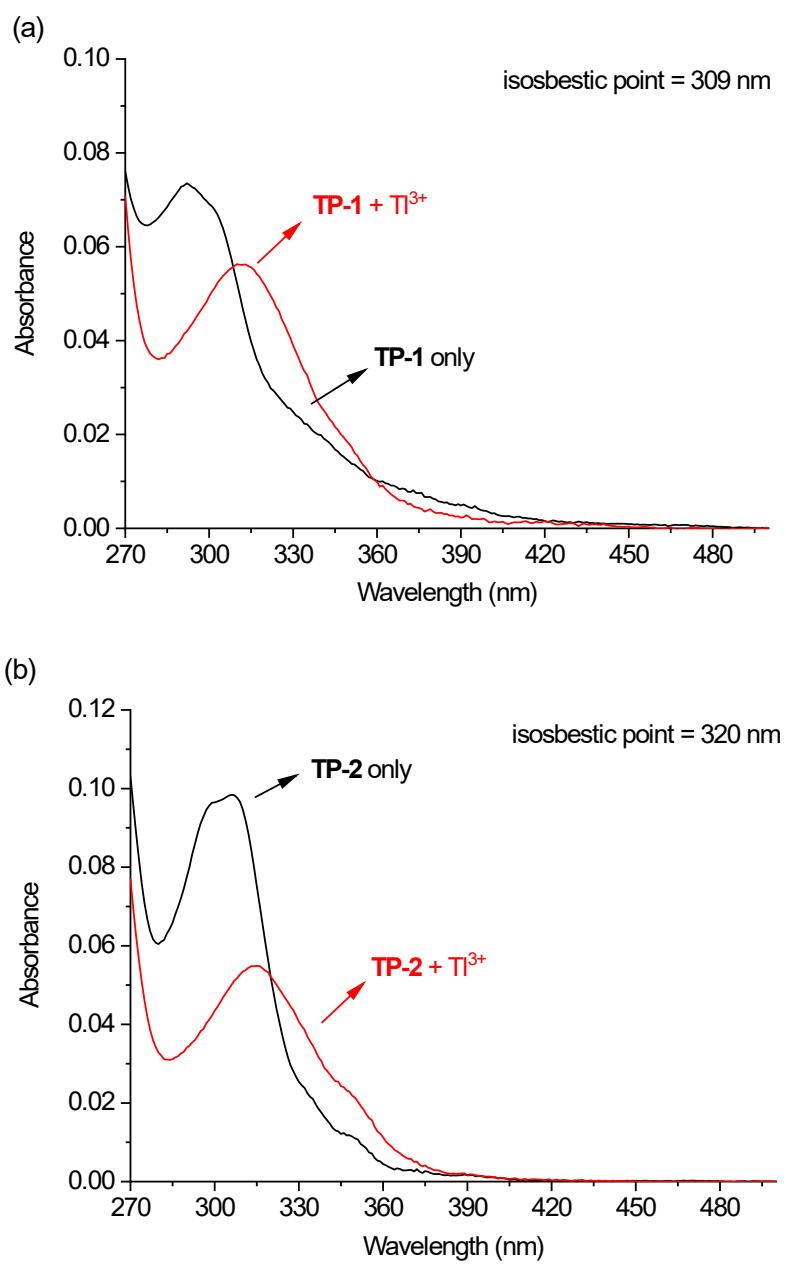


Fig. S1. UV-vis spectra of (a) TP-1 and (b) TP-2 in the presence and absence of Tl^{3+} . $[\text{TP-1}] = [\text{TP-2}] = 5.0 \mu\text{M}$, $[\text{Tl}^{3+}] = 50 \mu\text{M}$, in a pH 4.8 acetate buffer solution (10 mM) containing 1% (*v/v*) DMF.

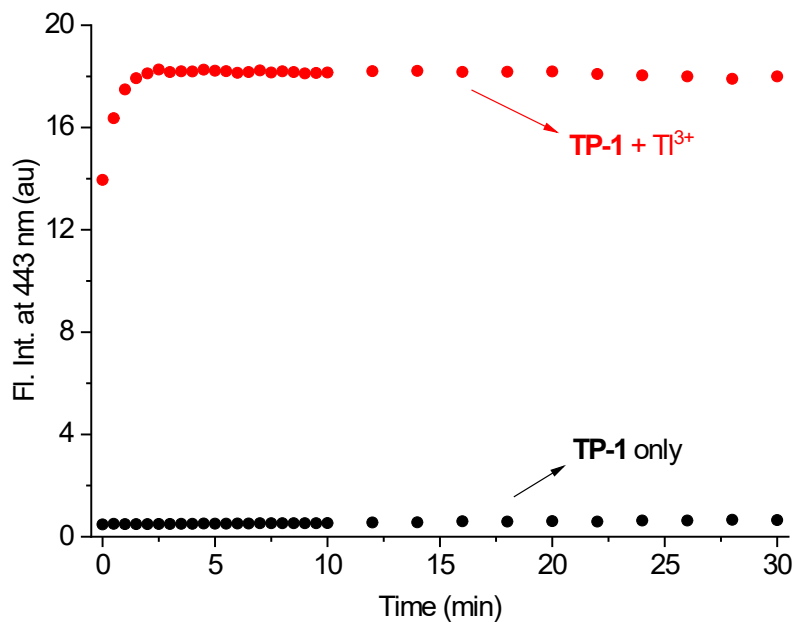


Fig. S2. Time-dependent fluorescence emission of **TP-1** at 443 nm in response to Tl³⁺. [TP-1] = 5.0 μM, [Tl³⁺] = 50 μM, in a pH 4.8 acetate buffer solution (10 mM) containing 1% (v/v) DMF. λ_{ex} = 309 nm.

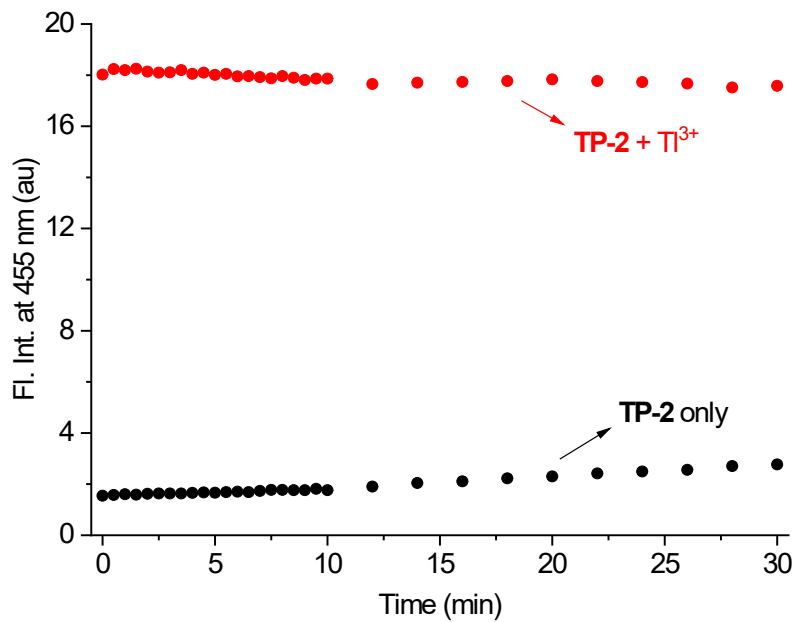


Fig. S3. Time-dependent fluorescence emission of **TP-2** at 455 nm in response to Tl³⁺. [TP-2] = 5.0 μM, [Tl³⁺] = 50 μM, in a pH 4.8 acetate buffer solution (10 mM) containing 1% (v/v) DMF. λ_{ex} = 320 nm.

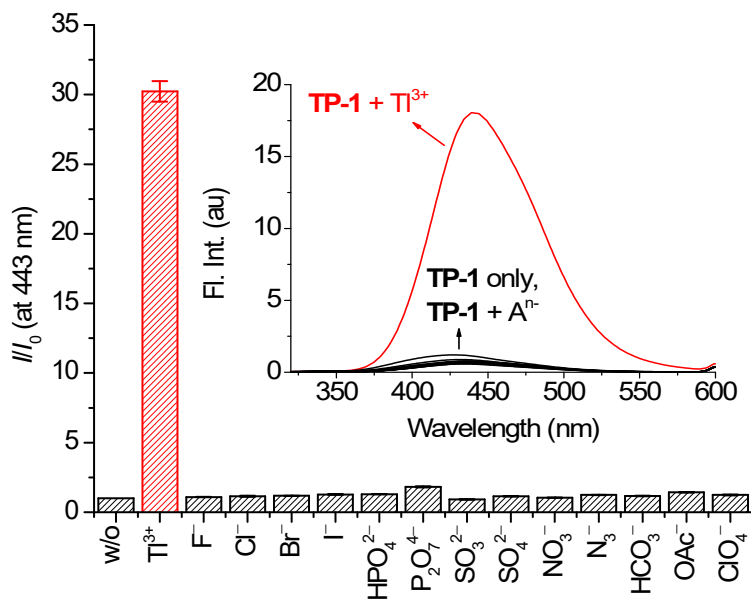


Fig. S4. Changes in fluorescence intensity enhancement (I/I_0) at 443 nm of **TP-1** in the presence of common anions. Inset: fluorescence spectra of **TP-1**. $[TP-1] = 5.0 \mu M$, $[Tl^{3+}] = [A^{n-}] = 50 \mu M$, in a pH 4.8 acetate buffer solution (10 mM) containing 1% (*v/v*) DMF. $\lambda_{ex} = 309 \text{ nm}$.

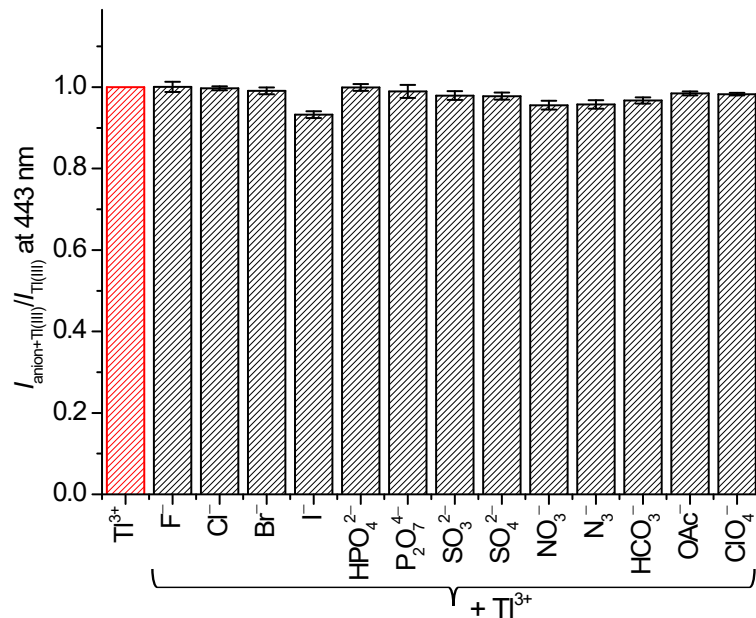


Fig. S5. Changes in fluorescence intensity ratio ($I_{\text{anion}+\text{Tl(III)}}/I_{\text{Tl(III)}}$) of **TP-1** at 443 nm in the presence of coexisting anions. $[TP-1] = 5.0 \mu M$, $[Tl^{3+}] = [A^{n-}] = 50 \mu M$, in a pH 4.8 acetate buffer solution (10 mM) containing 1% (*v/v*) DMF. $\lambda_{ex} = 309 \text{ nm}$.

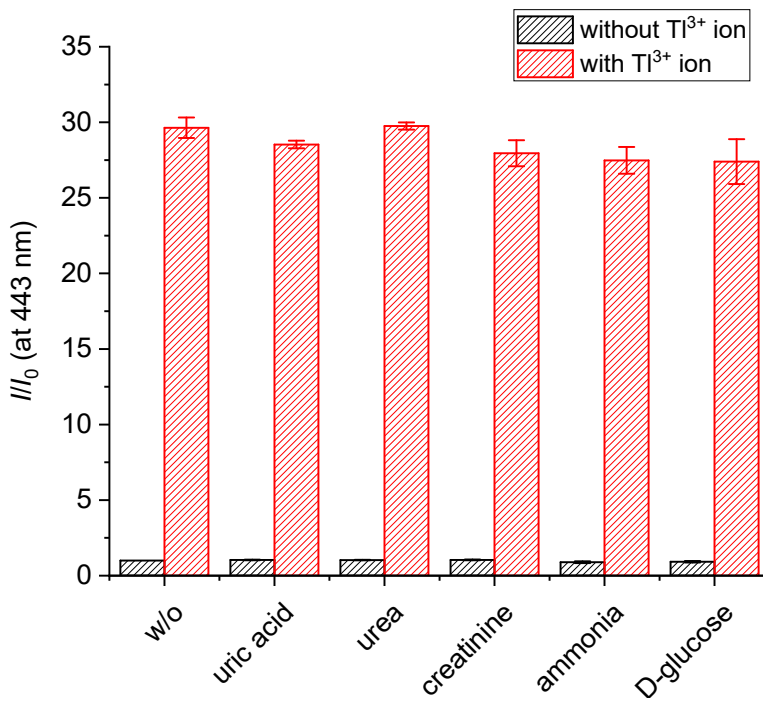


Fig. S6. Changes in fluorescence intensity enhancement (I/I_0) of **TP-1** at 443 nm in the presence of urine components. $[\text{TP-1}] = 5.0 \mu\text{M}$, $[\text{Tl}^{3+}] = [\text{urine component}] = 50 \mu\text{M}$, in a pH 4.8 acetate buffer solution (10 mM) containing 1% (*v/v*) DMF. $\lambda_{\text{ex}} = 309 \text{ nm}$.

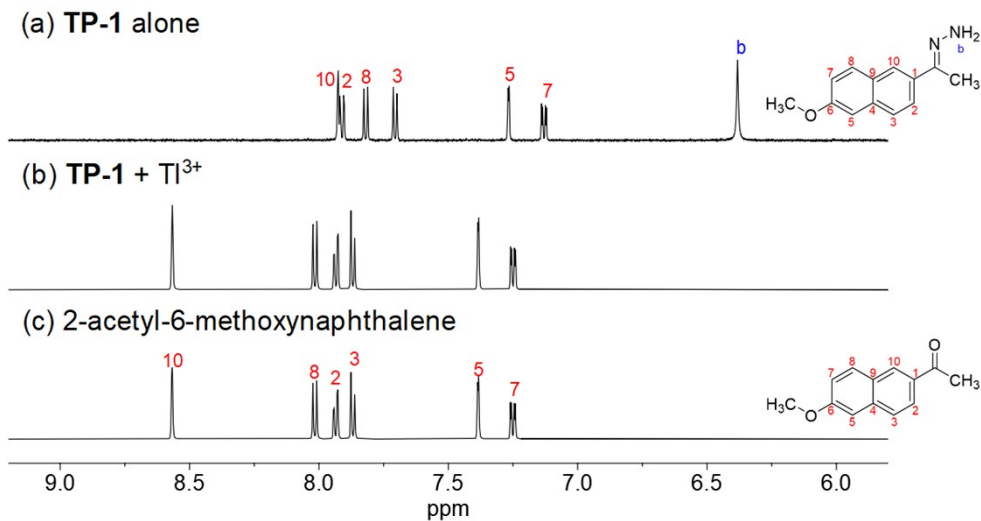


Fig. S7. Partial ^1H NMR spectra of (a) **TP-1**, (b) **TP-1 + Tl^{3+}** , and (c) 2-acetyl-6-methoxynaphthalene in $\text{DMSO}-d_6$. $[\text{TP-1}] = [2\text{-acetyl-6-methoxynaphthalene}] = 5.0 \text{ mM}$. For (b), the spectrum (**TP-1 + Tl^{3+}**) was obtained using a purified product of a mixture of **TP-1** (5.0 mM) and $\text{Tl}(\text{NO}_3)_3$ (10.0 mM) in acetate buffer solution (pH 4.8) containing 1% (*v/v*) DMF.

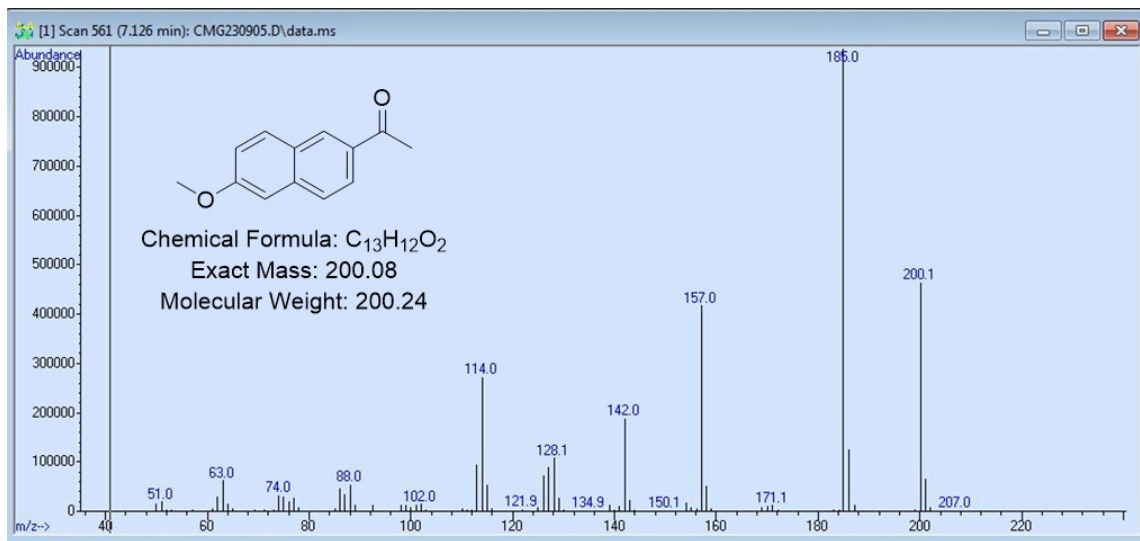


Fig. S8. Mass spectrum of the Tl³⁺ signaling product of **TP-1**.

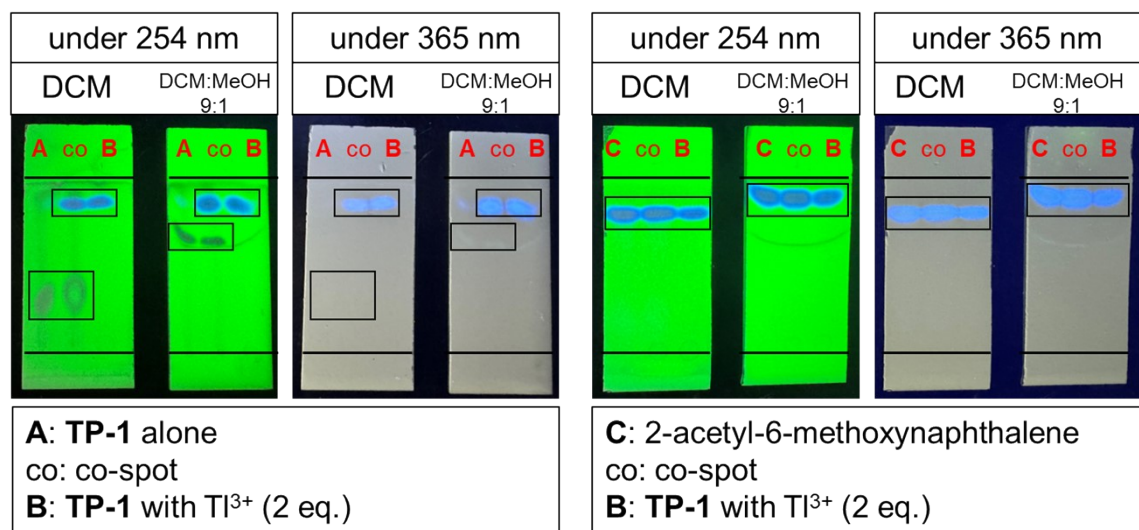


Fig. S9. TLC profile of **TP-1** (spot A), **TP-1** with Tl³⁺ (2.0 eq.) (spot B), and 2-acetyl-6-methoxynaphthalene (spot C).

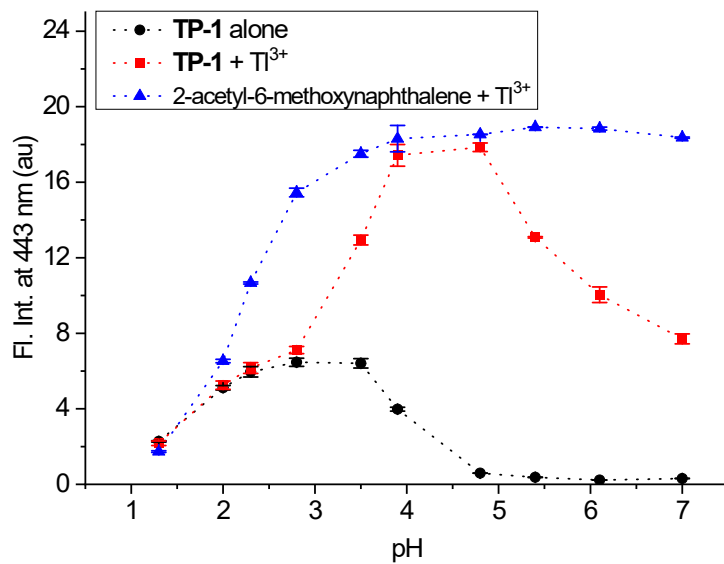


Fig. S10. Effect of pH on the Tl^{3+} signaling of **TP-1** expressed by changes in fluorescence intensity at 443 nm. $[\text{TP-1}] = [2\text{-acetyl-6-methoxynaphthalene}] = 5.0 \mu\text{M}$, $[\text{Tl}^{3+}] = 50 \mu\text{M}$, in a pH 4.8 acetate buffer solution (10 mM) containing 1% (*v/v*) DMF. HCl or NaOH solution was added to adjust the pH. $\lambda_{\text{ex}} = 309 \text{ nm}$.

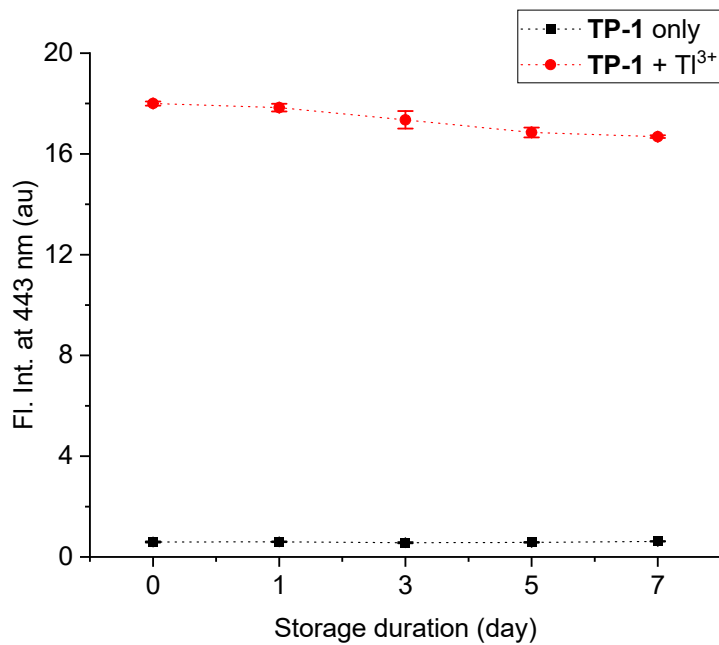


Fig. S11. Stability of **TP-1** stock solution over different storage durations. $[\text{TP-1}] = 5.0 \mu\text{M}$, $[\text{Tl}^{3+}] = 50 \mu\text{M}$, in a pH 4.8 acetate buffer solution (10 mM) containing 1% (*v/v*) DMF. The stock solutions were used after being stored for immediate use, 1 day, 3 days, 5 days, and 1 week at room temperature in the dark. $\lambda_{\text{ex}} = 309 \text{ nm}$.

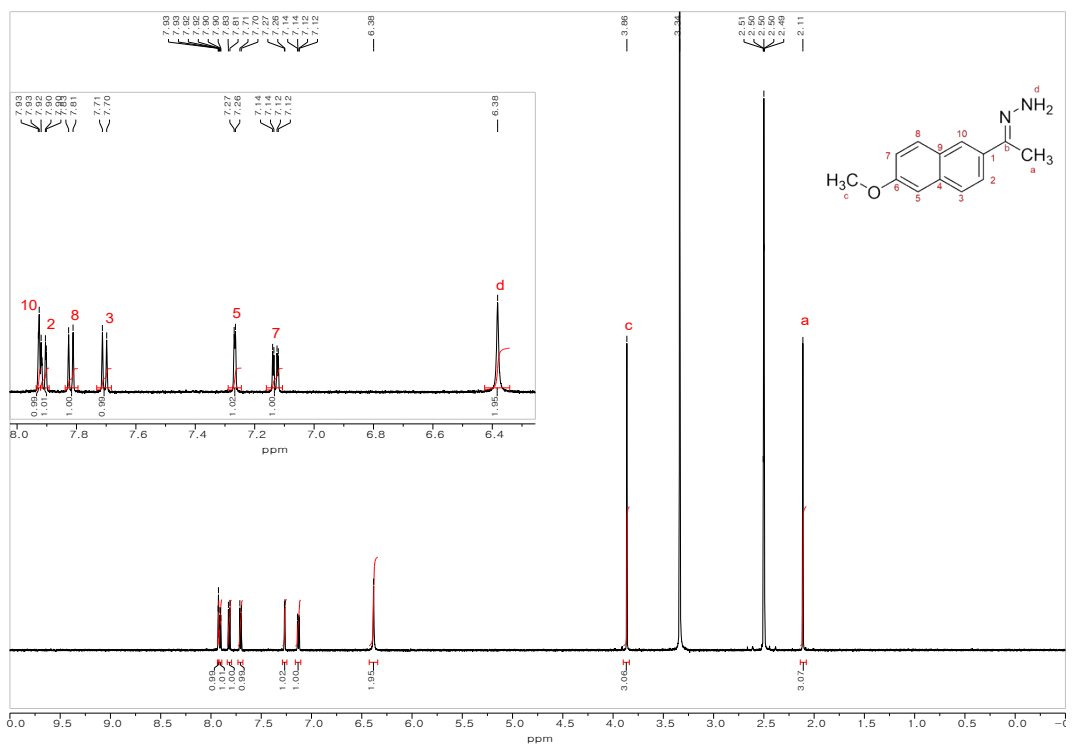


Fig. S12. ^1H NMR spectrum of TP-1 in $\text{DMSO}-d_6$ (600 MHz).

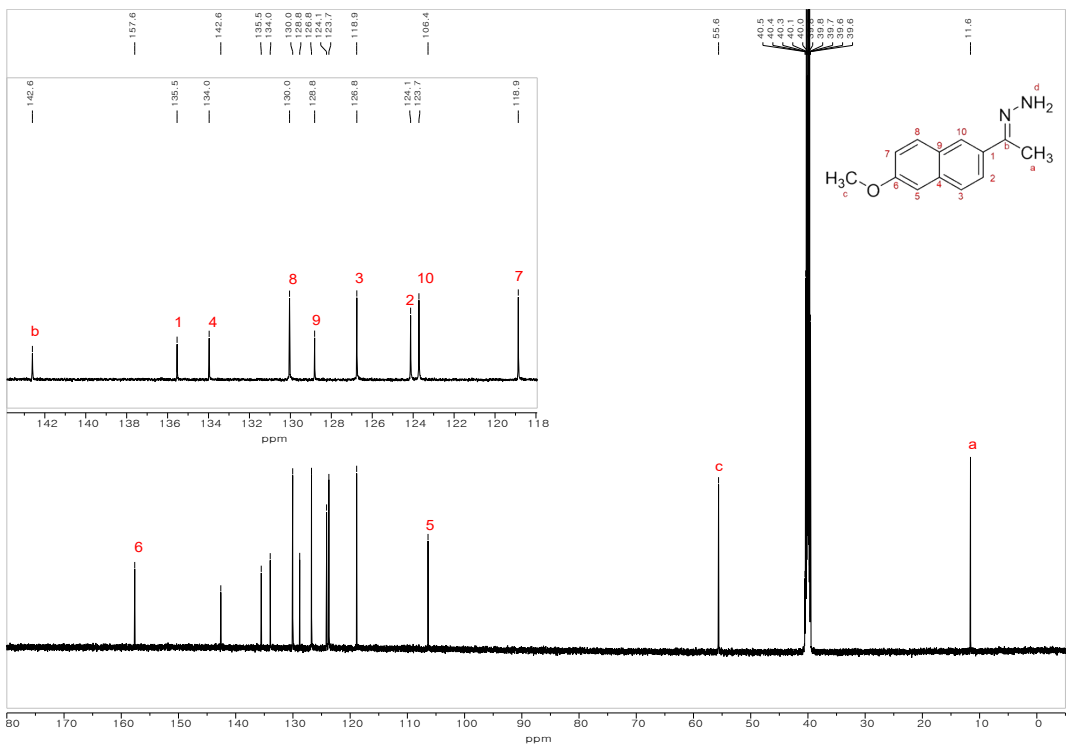


Fig. S13. ^{13}C NMR spectrum of TP-1 in $\text{DMSO}-d_6$ (150 MHz).

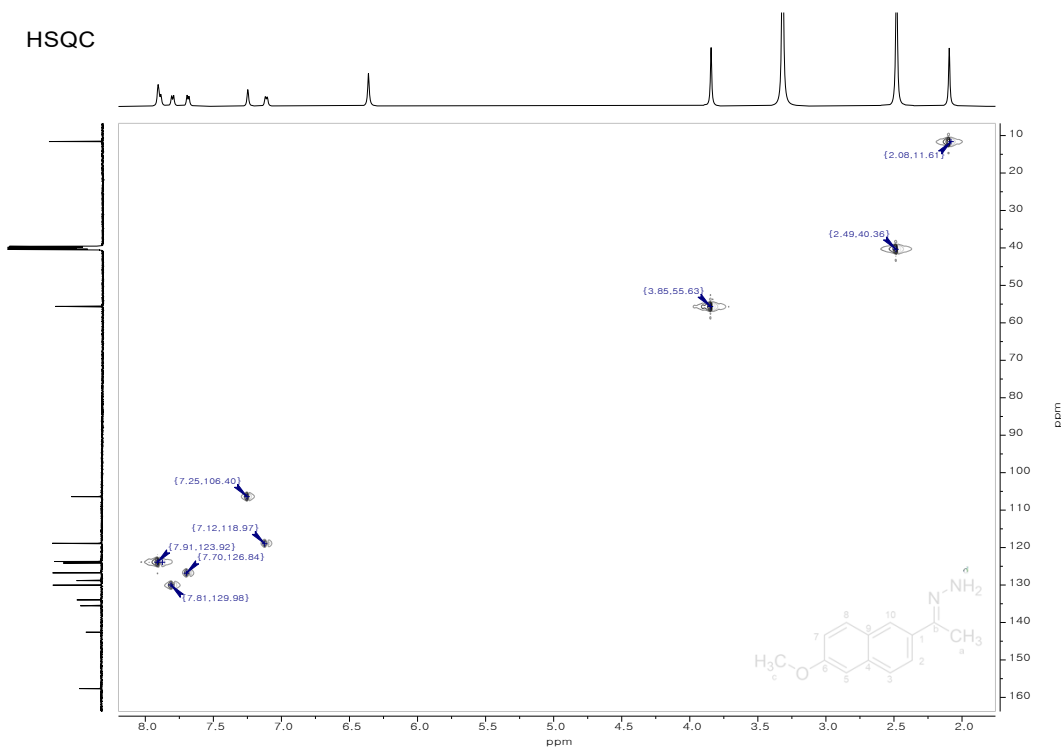


Fig. S14. HSQC NMR spectrum of TP-1 in $\text{DMSO}-d_6$.

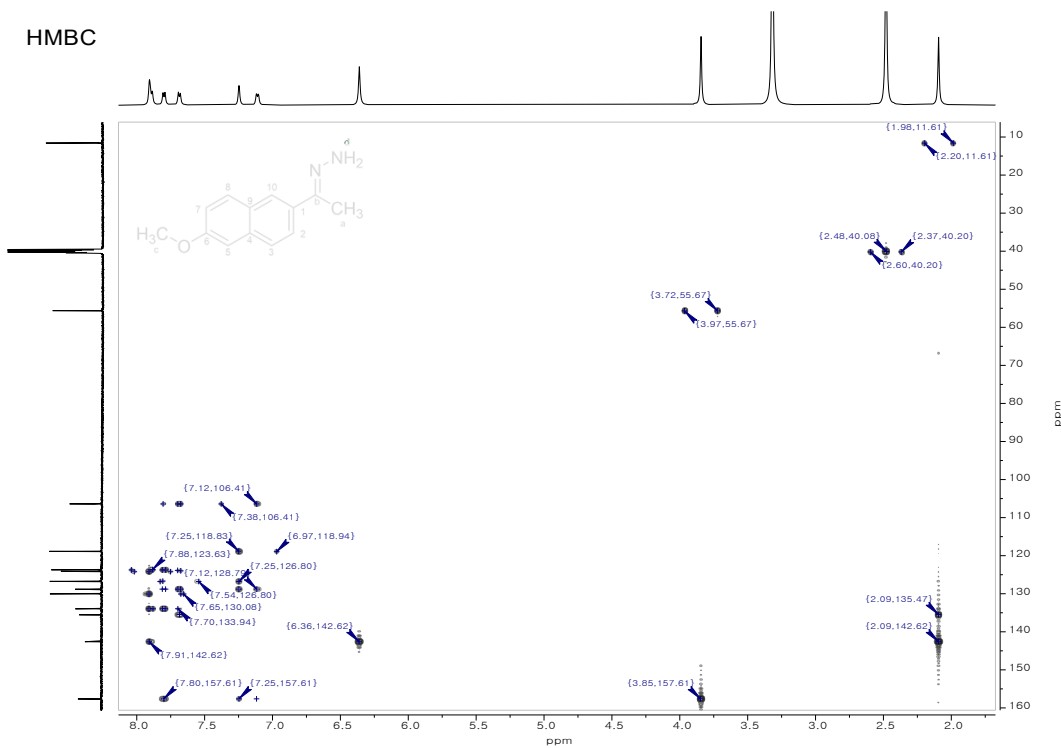


Fig. S15. HMBC NMR spectrum of TP-1 in $\text{DMSO}-d_6$.

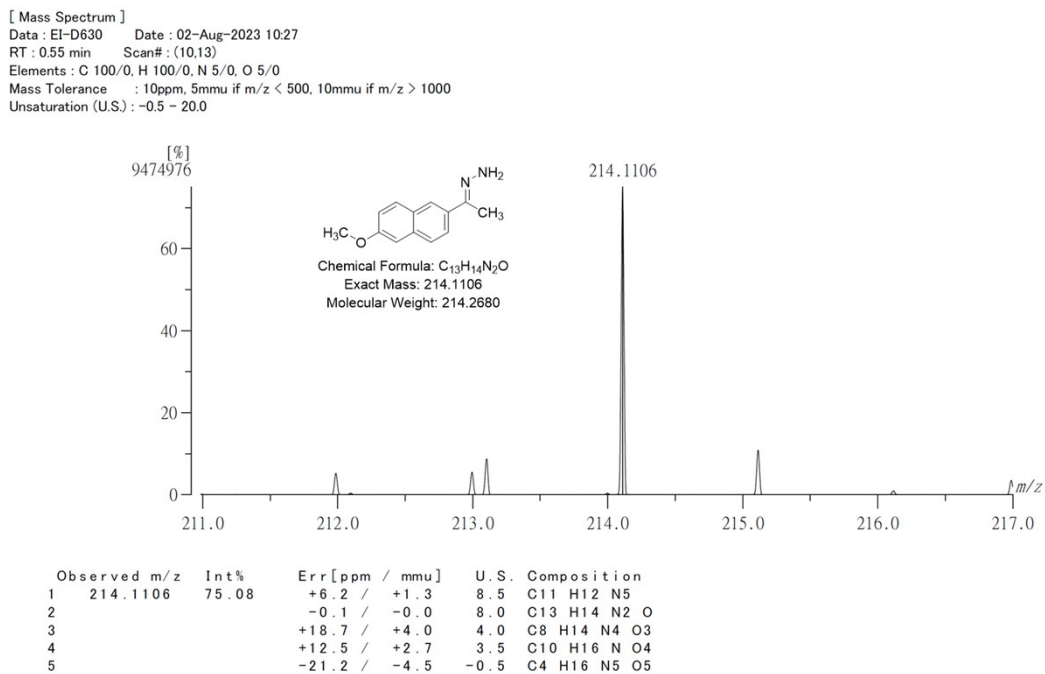


Fig. S16. High-resolution mass spectrum of TP-1.

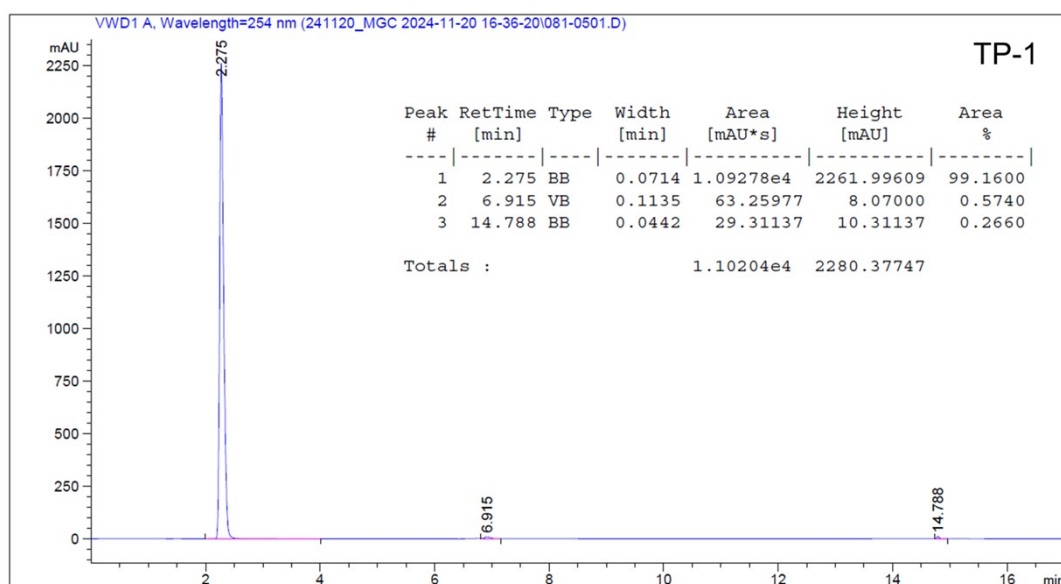


Fig. S17. HPLC chromatogram of TP-1. Column: C18 column, mobile phase: H₂O:CH₃CN = 8:2 (v/v), flow rate: 1 mL/min, detection: Abs at 254 nm.

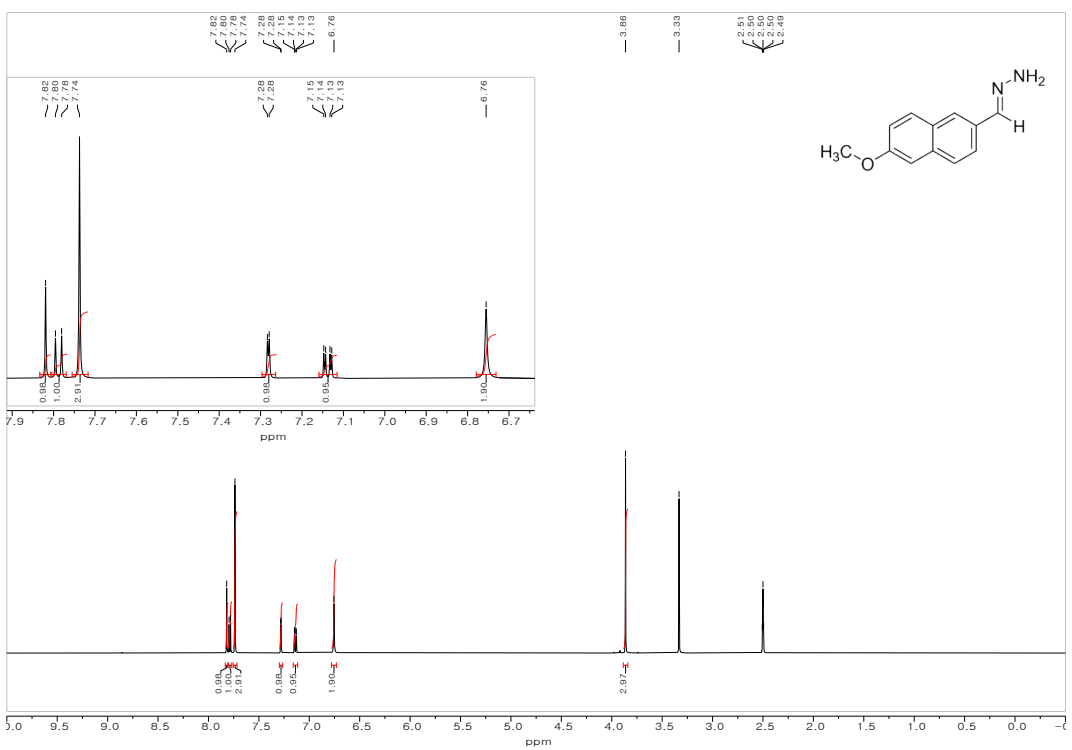


Fig. S18. ^1H NMR spectrum of TP-2 in $\text{DMSO}-d_6$ (600 MHz).

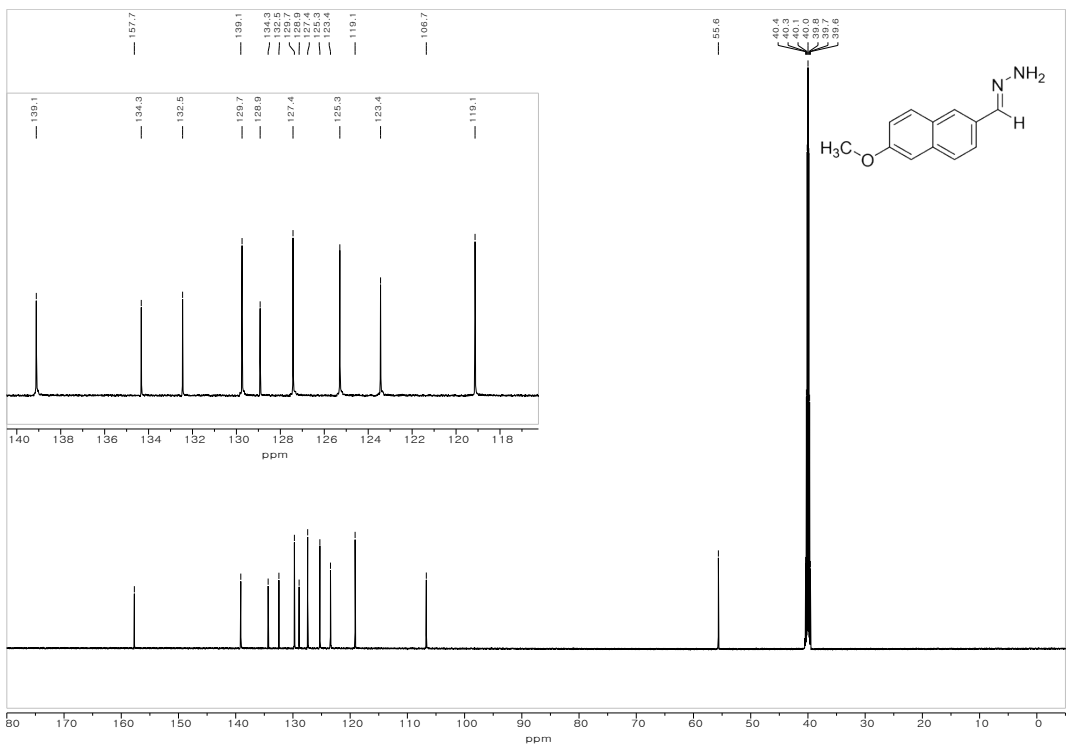


Fig. S19. ^{13}C NMR spectrum of TP-2 in $\text{DMSO}-d_6$ (150 MHz).

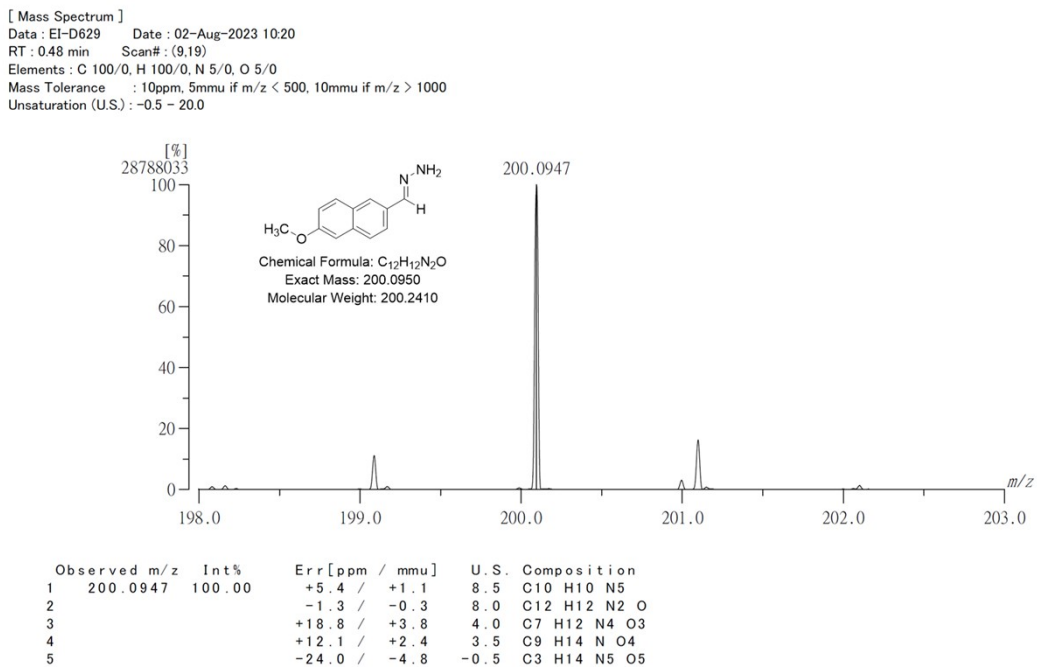


Fig. S20. High-resolution mass spectrum of TP-2.

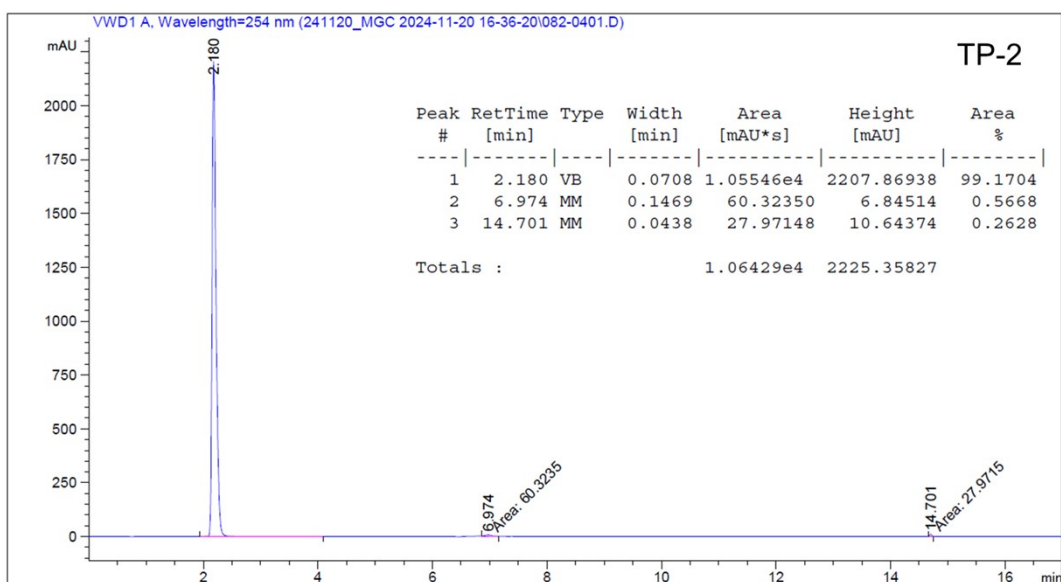


Fig. S21. HPLC chromatogram of TP-2. Column: C18 column, mobile phase: H₂O:CH₃CN = 8:2 (v/v), flow rate: 1 mL/min, detection: Abs at 254 nm.

References

- [S1] Y. K. Agrawal and V. J. Bhatt, *Analyst*, 1986, **111**, 761–765.
- [S2] B. Rezaei, S. Meghdadi and N. Majidi, *Spectrochim. Acta Part A*, 2007, **67**, 92–97.
- [S3] H. D. Revanasiddappa and T. N. K. Kumar, *Anal. Sci.*, 2002, **18**, 1131–1135.
- [S4] S. Ge, P. Dai, J. Yu, Y. Zhu, J. Huang, C. Zhang, L. Ge and F. Wan, *Intern. J. Environ. Anal. Chem.*, 2010, **90**, 1139–1147.
- [S5] P. Nagaraja, N. G. S. Al-Tayar, A. Shivakumar, A. K. Shresta and A. K. Gowda, *J. Mex. Chem. Soc.*, 2009, **53**, 201–208.
- [S6] Y. J. Lee, M. G. Choi, J. H. Yoo, T. J. Park, S. Ahn and S.-K. Chang, *J. Photochem. Photobiol. A*, 2020, **394**, 112471.
- [S7] J. H. Yoo, Y. J. Lee, K. M. Lee, M. G. Choi, T. J. Park and S.-K. Chang, *New J. Chem.*, 2021, **45**, 603–609.
- [S8] W. H. Melhuish, *J. Phys. Chem.*, 1961, **65**, 229–235.